ACADEMIC PRESS

Available online at www.sciencedirect.com

SCIENCE DIRECT®

NeuroImage 18 (2003) 214–230

NeuroImage

www.elsevier.com/locate/ynimg

The relationship between changes in intrinsic optical signals and cell swelling in rat spinal cord slices

Eva Syková,* Lýdia Vargová, Šárka Kubinová, Pavla Jendelová, and Alexandr Chvátal

Department of Neuroscience, 2nd Medical Faculty, Charles University, Institute of Experimental Medicine, Academy of Sciences of the Czech Republic, and Center for Cell Therapy and Tissue Repair, Prague, Czech Republic

Received 23 January 2002; revised 16 August 2002; accepted 13 September 2002

Abstract

Changes in intrinsic optical signals could be related to cell swelling; however, the evidence is not compelling. We measured light transmittance, ECS volume fraction (α), and extracellular K^+ in rat spinal cord slices during electrical stimulation and the application of elevated potassium, NMDA, or anisoosmotic solutions. Dorsal root stimulation (10 Hz/1 min) induced an elevation in extracellular K^+ to 6–8 mM, a light transmittance increase of 6–8%, and a relative ECS volume decrease of less than 5%; all of these changes had different time courses. The application of 6 or 10 mM K^+ or NMDA (10^{-5} M) had no measurable effect on α, but light transmittance increased by 20–25%. The application of 50 or 80 mM K^+ evoked a 72% decrease in α while the light transmittance increase remained as large as that in 6 or 10 mM K^+. While the change in α persisted throughout the 45-min application, light transmittance, after peaking in 6–8 min, quickly returned to control levels and decreased below them. Astrocytic hypertrophy was observed in 6, 10, and 50 mM K^+. The same results followed the application of 10^{-4} M NMDA or hypotonic solution (160 mmol/kg). The elevation of extracellular K^+ after NMDA application, corresponding to increased neuronal activity, had a similar time course as the light transmittance changes. Furosemide, Cl^--free, or Ca^{2+}-free solution blocked or slowed down the decreases in α, while the light transmittance increases were unaffected. In hypertonic solution (400 mmol/kg), α increased by 30–40%, while light transmittance decreased by 15–20%. Thus, light transmittance changes do not correlate with changes in ECS volume but are associated with neuronal activity and morphological changes in astrocytes.

Keywords: Astrocytes; Extracellular space volume; Extracellular potassium; GFAP; Hypertrophied astrocytes; Light transmittance; Tortuosity

Introduction

Light scattering in living tissue results from refractive index inhomogeneities. These generate intrinsic optical signals that result from changes in the structural properties of the tissue. Changes in intrinsic optical signals, studied by light transmitted through the tissue, result not only from light scattering (refraction and reflection) but also from light absorption. As suggested more than 30 years ago (Cohen et al., 1968, 1972a,b), there are various mechanisms that might be involved in intrinsic optical signal changes during physiological stimulation or pathological states.

Changes in light scattering and light reflectance in brain slices have been described in many situations in mammalian brain in vivo as well as in vitro: during stimulation-evoked neuronal activity, extracellular potassium accumulation, hypotonic stress, oxygen/glucose deprivation, exposure to glutamate receptor agonists, and spreading depression (MacVicar and Hochman, 1991; Andrew and MacVicar, 1994; Kreisman et al., 1995; Andrew et al., 1996; Murase et al., 1998; Jarvis et al., 1999; Müller and Somjen, 1999; Rector et al., 1997; Rector et al., 2001; Asai et al., 2002; Fayuk et al., 2002). These manipulations lead to numerous changes, all of which can change intrinsic optical signals, e.g., depolarization of neurons and glia, altered blood flow, hemoglobin oxidation, cytochrome reduction, osmotic changes, cell damage or death, astrogliosis, cell swelling, and changes in membrane configuration, cellular organelles,

* Corresponding author. Department of Neuroscience, Institute of Experimental Medicine ASCR, Videňská 1083, 142 20 Prague 4, Czech Republic. Fax: +420-296-442-782.

E-mail address: sykova@biomed.cas.cz (E. Syková).

1053-8119/03/$ – see front matter © 2003 Elsevier Science (USA). All rights reserved.
PII: S1053-8119(02)00014-9

cell shape, protein condensation, extracellular matrix, and extracellular space (ECS) volume and geometry (Jarvis et al., 1999; Syková et al., 2000; Syková, 2001).

In vivo, three components can be distinguished in the intrinsic optical signal activity-related response, each of which has a maximum at a different wavelength. The first two components are attributable to changes in blood volume and oxygen consumption, the third to light scattering signals. In vitro, only the component based on scattered light, which is wavelength-independent, can be observed (Grinvald et al., 1988).

The recently favored hypothesis is that changes in intrinsic optical signals are related to a water shift from the extra- to the intracellular compartment and can therefore be correlated with a decreased ECS volume due to activity-related cell swelling (MacVicar and Hochman, 1991; Tasaki and Byrne, 1993; Kreisman et al., 1995; Holthoff and Witte, 1998). However, there is no compelling evidence so far that changes in intrinsic optical signals correspond only to cell volume changes. More than 50 years ago, Hill and Keynes (1949) showed that light scattering in neuronal tissue changes during activation, and Cohen and Keynes (1968) proposed that light scattering originates from at least two different phenomena: cellular swelling and membrane conformation changes. Recently, Jarvis et al. (1999) proposed that changes in light transmittance are a more complex phenomenon, generated by alterations to neuronal and glial structure, and that initial light transmittance changes presumably caused by cell swelling are overridden by changes in dendritic conformation due to acute somatic and dendritic damage during excitotoxic stress. It is therefore evident that the mechanism(s) of intrinsic optical signal changes in various situations is far from clear.

Cell swelling or an ECS volume decrease has not yet been measured simultaneously with intrinsic optical signal changes in such a way that a definitive conclusion about the contribution of water shifts to light transmittance can be made. We therefore studied changes in light transmittance in rat spinal cord slices evoked by dorsal root stimulation as well as by increased potassium, osmotic stress, and the glutamate receptor agonist NMDA. In contrast to stimulation, which leads to relatively very small changes in ECS volume (Svoboda and Syková, 1991; Prokopová-Kubinová and Syková, 2000), these other manipulations have been shown to lead to more significant cell swelling and compensatory ECS volume decrease (Syková et al., 1999; Vargová et al., 2001). We used cell swelling and neuronal activity inhibitors and procedures that evoked light transmittance changes without inducing any apparent cell swelling. Simultaneously with light transmittance, we measured three extracellular space diffusion parameters using the real-time iontophoretic TMA^+ method: ECS volume fraction α = ECS volume/total tissue volume, ECS tortuosity $\lambda = (D/ADC)^{0.5}$, where D is the free diffusion coefficient and ADC is the apparent diffusion coefficient in the tissue, and nonspecific uptake k' (Nicholson and Phillips, 1981; Nicholson and Syková, 1998). The TMA^+ method is the only method that, if appropriately used, can provide absolute values of all three ECS diffusion parameters. ECS volume fraction is related to cell swelling, while tortuosity is often increased by structural changes, particularly astrocytic hypertrophy, and increases in extracellular matrix (Syková et al., 1998; Roitbak and Syková, 1999; Vargová et al., 2001). To study whether the observed changes in light transmittance are related to ongoing neuronal activity, we measured the activity-related increase in extracellular potassium concentration ($[K^+]_e$), using K^+-selective microelectrodes. The increase in $[K^+]_e$ has been shown to be proportional to the frequency and duration of neuronal activity (for review see Syková, 1983; Syková, 1992). In addition, we studied morphological changes in astrocytes.

Material and methods

Spinal cord slice preparation and solutions

The study was performed on 76 Wistar rat pups, 9–11 days old. After decapitation performed under ether anesthesia, the lumbal part of the spinal cord was isolated in a chamber with cold (8°C) artificial cerebrospinal fluid of the following composition (in mM): NaCl, 117.0; KCl, 3.0; $NaHCO_3$, 35.0; Na_2HPO_4, 1.25; D-glucose, 10.0; $MgCl_2$, 1.3; $CaCl_2$, 1.5 (pH 7.3). Four hundred micrometer thick transversal slices were cut on a vibratome (Electron Microscopy Sciences, USA). In experiments with electrical stimulation, 500-μm thick spinal cord slices were cut with attached dorsal roots. The solution was saturated with 95% O_2 and 5% CO_2. The slice was put in a small chamber, weighted at the edges using a U-shaped silver wire with nylon threads, and kept submerged in perfusion solution in the imaging chamber, continuously perfused at a rate of 5 ml/min. The temperature in the chamber was increased during 1 h to 21–22°C. The osmolarity of the artificial cerebrospinal fluid was 300 mmol/kg. In stimulation experiments, the dorsal roots were stimulated supramaximally (10 Hz for 1 min, rectangular pulses of 6–10 V, duration 0.1 ms) through a suction electrode.

Solutions with an increased concentration of K^+ (6, 10, 20, 50, or 80 mM) or Mg^{2+} (20 mM) contained reciprocally reduced Na^+ concentrations to maintain isoosmolarity. The glutamate receptor agonist NMDA was used at concentrations of 10^{-5} or 10^{-4} M. Ca^{2+}-free solutions were prepared by omitting $CaCl_2$ and adding 1 mM EGTA; furosemide was dissolved in the perfusing solution at a concentration of 2 mM. The osmotic strength of the solutions was kept constant at 300 mmol/kg and was measured using a vapor pressure osmometer (Vescor, Logan, UT). Hypoosmotic solutions with an osmolality of either 200 mmol/kg (H200) or 160 mmol/kg (H160) were prepared by reducing the NaCl content. To evoke cell shrinkage, we used a hyperosmotic solution with an osmolarity of 400 mmol/kg (H400)

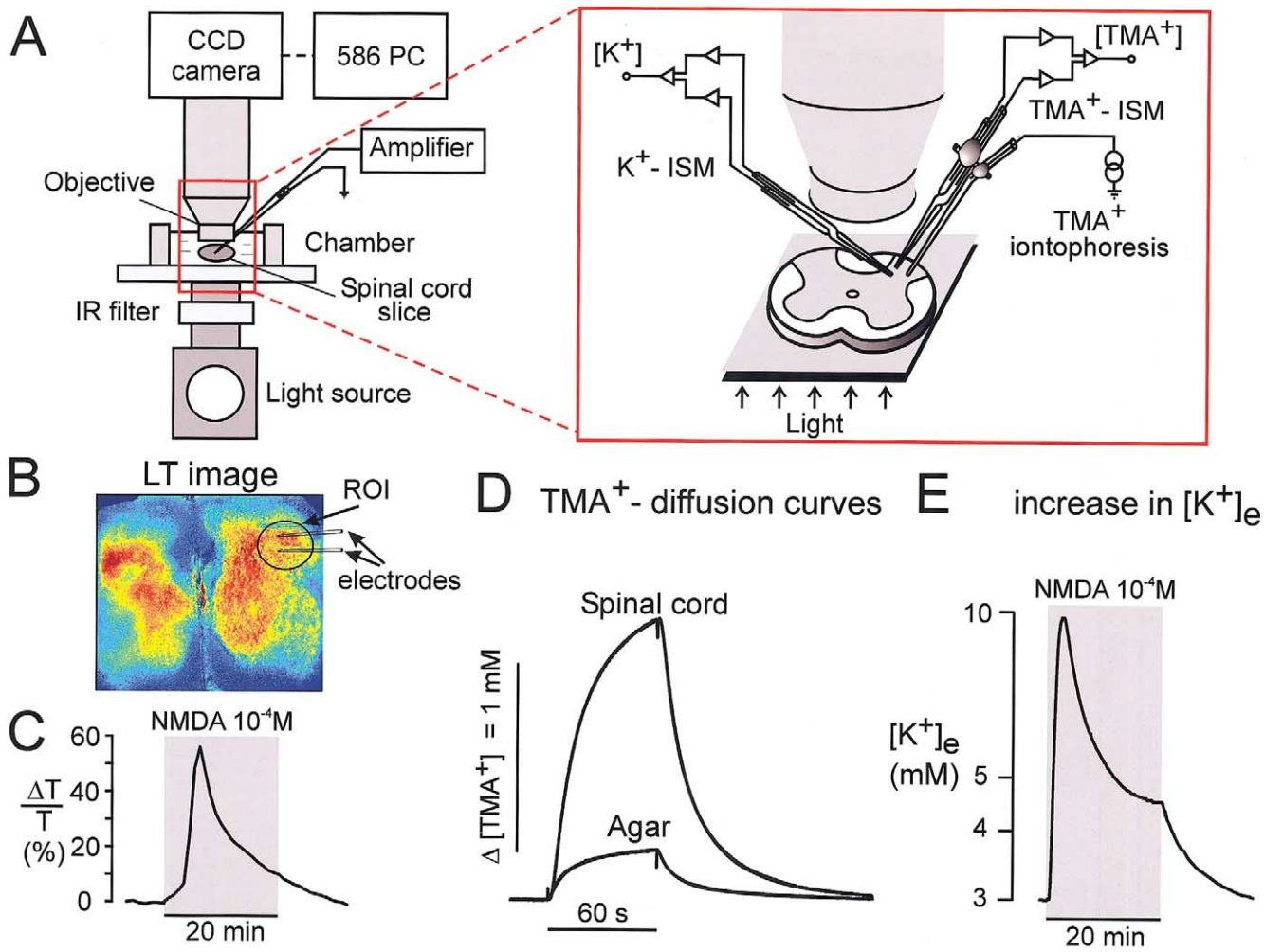

Fig. 1. Experimental arrangement for the simultaneous measurement of light transmittance, ECS diffusion parameters and/or changes in extracellular K^+ concentration ($[K^+]_e$). (A) Ion-sensitive microelectrodes (ISM) were inserted into the dorsal horns of spinal cord slices fixed by a U-shaped platinum wire with a nylon grid in a perfusion chamber mounted on the stage of a fluorescence microscope (Axioskop FX, Carl Zeiss, Germany). (B) Example of changes in light transmittance (LT) evoked by a 20-min application of 10^{-4} M NMDA. The pseudocolor image reflects the spatial distribution of the percentage of change in light transmittance 5 min after the onset of the application. The time course of light transmittance changes, expressed as the percentage of change ($\Delta T/T\%$) in the area of the dorsal horn selected as the region of interest (ROI), is shown in C. (D) Typical recordings of TMA^+ diffusion curves in agar and in spinal cord gray matter during perfusion with artificial cerebrospinal fluid. (E) Typical recording of an increase in $[K^+]_e$ evoked by 10^{-4} M NMDA application. For further explanation, see Material and methods.

with added sucrose. All substances were purchased from Sigma (Prague).

Experiments were carried out in accordance with the European Communities Council Directive of 24 November 1986 (86/609/EEC).

Measurements of light transmittance

The experimental setup for optical imaging, ECS diffusion parameter measurements using TMA^+-selective microelectrodes, and extracellular potassium measurements using

Fig. 2. Effect of dorsal root stimulation on changes in light transmission (LT), $[K^+]_e$ and TMA^+ baseline in the spinal dorsal horn. (A) Video images of LT changes in spinal cord dorsal horn taken at 15-s intervals during and after tetanic (10 Hz/1 min) stimulation of the dorsal root. (B) The time course and spatial distribution of LT changes. Each time course was a spatial average of the selected region of interest (ROI) indicated by circles a–l. The LT increase was most intense within Rexed's laminae II–III. After the end of stimulation, LT in lamina II decreased below the control value, whereas LT in laminae IV and V decreased slowly and remained elevated for several minutes. (C) The time courses of stimulation-induced changes in LT and TMA^+ and $[K^+]_e$ concentrations. The time courses were measured in regions indicated in Fig. 2B as ROI e and h. An increase in TMA^+ concentration indicated a relative decrease in ECS volume of about 5%. Note that the TMA^+ concentration increases as well as their decay were faster than the changes in LT. The stimulation-induced $[K^+]_e$ concentration increase reached a maximum within the first 5 s and then $[K^+]_e$ returned to control levels.

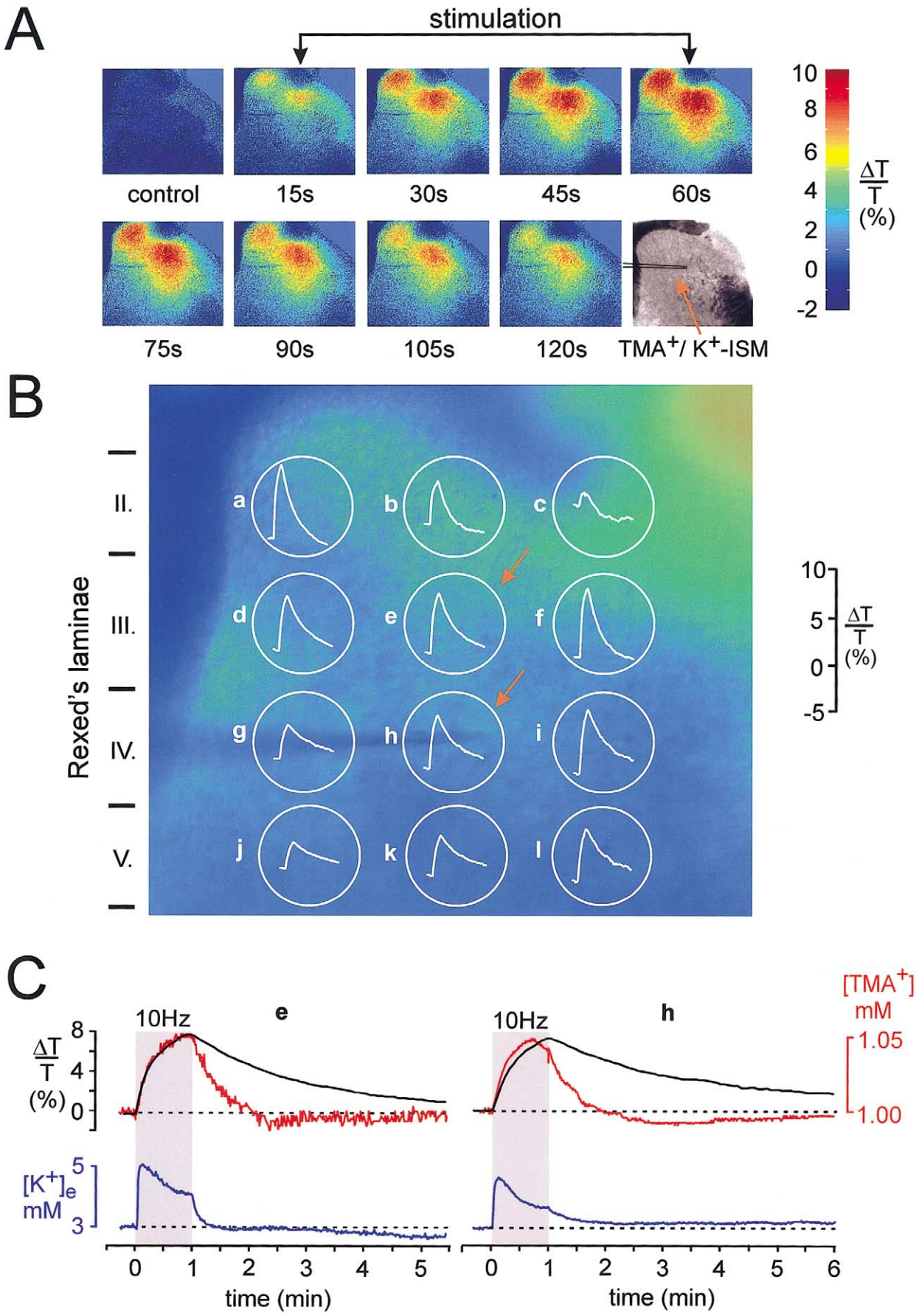
A
stimulation
control
15s
30s
45s
60s
75s
90s
105s
120s
TMA+/ K+-ISM
10
8
6
4
2
0
-2
ΔT/T (%)
B
Rexed's laminae
II.
III.
IV.
V.
a
b
c
d
e
f
g
h
i
j
k
l
10
5
0
-5
ΔT/T (%)
C
10Hz
e
10Hz
h
ΔT/T (%)
8
4
0
[K+]e mM
5
3
[TMA+] mM
1.05
1.00
0
1
2
3
4
5
6
time (min)

K^+-selective microelectrodes is illustrated in Fig. 1. For the light transmittance measurements, slices were transilluminated with light of a near-infrared wavelength (650 nm), and video images were acquired with a CCD camera (SenSys 1400, Photometrics) and processed using Axon Imaging Workbench software. The CCD output was linear with respect to the change in light intensity. During stimulation, a series of images of the dorsal spinal horn was acquired at the rate of 1 image every 2 s. In order to obtain high resolution images of long-lasting changes in light transmittance in the entire spinal cord slice in response to hypotonic solution, high potassium, or NMDA application, a series of whole slice images was acquired at the rate of 1 image every minute. This slow rate was still sufficient for the accurate determination of changes in light transmittance. The software used for optical signal analysis uses only a single control image subtracted from all experimental images and does not allow baseline shift correction. Therefore, a control recording lasting at least 10 min was done before each application, and a stimulus was applied only if the baseline variation did not exceed ±1.0%. Data acquisition was begun only if the light transmittance baseline was stable. The control image (T_{cont}) was subtracted from each experimental image (T_{exp}). The change in light transmittance (LT) was expressed as the difference in image intensity ($T_{exp} - T_{cont}$) in the selected area. To normalize the data from all experiments, this value was then expressed as the percentage change of the intensity in the area using the following equation:

$$LT = \left(\frac{T_{exp} - T_{cont}}{T_{cont}}\right) \times 100 = \frac{\Delta T}{T}\%.$$

The calculated percentage change of light transmittance in each pixel of the image was used to create a pseudocolor image by the program MATLAB (Fig. 1B). Regions of interest were selected in the dorsal horns of the spinal cord slices in the area surrounding the insertion point of the TMA^+- and/or K^+-sensitive microelectrodes. The time course of light transmittance changes (Fig. 1C) was subsequently compared with those of changes in ECS volume and $[K^+]_e$ (Fig. 1E).

Measurements of K^+ increase, and TMA^+ baseline and diffusion parameters in the extracellular space

To measure diffusion parameters in the extracellular space (ECS), the real-time iontophoretic method originally developed by Nicholson and Phillips (1981) and described in our previous studies (Lehmenkühler et al., 1993; Syková et al., 1994; Syková et al., 1999) was used. In brief, an extracellular marker such as tetramethylammonium ions (TMA^+), to which cell membranes are relatively impermeable, is administered into the nervous tissue by iontophoresis. The concentration of TMA^+ is measured in the ECS by a TMA^+-selective microelectrode (TMA^+-ISM) and is inversely proportional to the ECS volume. Double-barreled TMA^+-ISMs were prepared by the procedure described in Syková (1992). The liquid ion-exchanger highly sensitive to TMA^+ was Corning 477317. The TMA^+-sensitive barrel of the microelectrode was backfilled with 100 mM TMACl, while the reference barrel contained 150 mM NaCl. Iontophoretic micropipettes were pulled from theta glass (Clark Electrochemical Instruments, England). Before backfilling with 0.1 M TMA^+, the shank of the electrode was bent so that it could be aligned parallel to the TMA^+-ISM. To stabilize the intertip distance (100–180 μm), both electrodes were glued together with dental cement (Fig. 1). Typical iontophoresis parameters were a +20 nA bias current (continuously applied to maintain a constant transport number) and a +200 nA current step of 60 s duration to generate the diffusion curve. TMA^+ diffusion curves were superimposed on a TMA^+ baseline corresponding to the TMA^+ concentration in the perfusate plus the applied bias current, which increased the TMA^+ baseline to 0.28–0.32 mM, captured on a digital oscilloscope (Nicolet 310), transferred to a PC-compatible computer, and analyzed to yield the volume fraction α, tortuosity λ, and nonspecific uptake k' using the program VOLTORO (kindly provided by C. Nicholson).

TMA^+ diffusion curves were first recorded in 0.3% agar gel (Difco, Special Noble Agar) dissolved in a solution of 150 mM NaCl, 3 mM KCl, and 1 mM TMACl, in which by definition $\alpha = 1 = \lambda$ and $k' = 0$ (free-diffusion values). The obtained diffusion curves were analyzed by fitting the data using a nonlinear curve-fitting simplex algorithm to yield the iontophoretic electrode transport number (n) and free diffusion coefficient for TMA^+ (D). The electrode array was then lowered into a spinal cord slice to a depth of 200–300 μm, and diffusion curves were recorded in dorsal horn gray matter (Fig. 1). Knowing n and D, the ECS diffusion parameters α, λ, and k' were calculated from modified diffusion equations (Nicholson and Phillips, 1981; Nicholson and Syková, 1998). The time course of a decrease in α corresponds well with the time course of changes in TMA^+ baseline concentration. The calculation of the absolute values of the diffusion parameters cannot, however, be made faster than every 3–5 min. To detect small and fast volume changes associated with physiological activation during stimulation, relative changes in ECS volume were determined by measuring changes in TMA^+ baseline concentration. For measurements of TMA^+ baseline, artificial cerebrospinal fluid containing 1 mM TMA chloride was used. Changes in TMA^+ baseline concentration can be interpreted as relative changes in ECS volume using the following expression (Svoboda and Syková, 1991):

$$\text{changes of ECS volume (\%)} = (1 - [TMA^+] \text{ before stimulation}/[TMA^+] \text{ during stimulation}) \times 100.$$

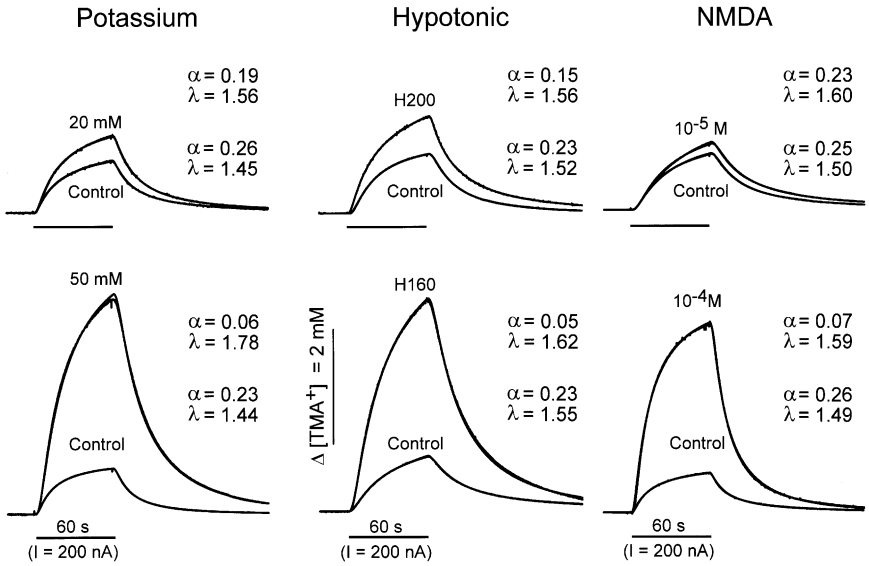

Fig. 3. The effect of increased K^+ concentration (20 or 50 mM), hypotonic solutions (200 or 160 mmol/kg), or NMDA (10^{-5} or 10^{-4} M) on ECS diffusion curves recorded in spinal dorsal horn. Values of α and λ are shown with each diffusion curve.

Extracellular K^+ concentration ($[K^+]_e$) was recorded by means of double-barreled K^+-selective microelectrodes (K^+-ISM) prepared similarly as TMA^+-ISM (Fig. 1); however, the K^+-sensitive barrel of the microelectrode was backfilled with 0.5 M KCl (see Syková, 1992). The K^+-ISMs were calibrated in solutions containing 3, 6, 8, 10, 20, or 50 mM KCl in 150 mM NaCl.

Immunohistochemistry

Slices were perfused and incubated in the same solutions as for electrophysiological experiments. Subsequently, the slices were fixed in 4% paraformaldehyde in 0.1 M phosphate-buffered saline (PBS; pH 7.5). Fixed slices were immersed in PBS with 30% sucrose. Frozen transversal spinal cord sections (40 μm) were cut through the lumbar part. Astrocytes were identified using monoclonal antibodies to glial fibrillary acidic protein (GFAP, Boehringer-Mannheim, Mannheim, Germany). GFAP antibodies were diluted 1:20 in PBS containing 1% bovine serum albumin (BSA, Sigma) and 0.2% Triton X-100. Following overnight incubation in the primary antibody at 4°C, the floating sections were washed and processed using a biotinylated anti-mouse secondary antibody and the avidin–biotin peroxidase complex method (Vectastain Elite, Burlingame, USA). Immune complexes were visualized using 0.05% 3,3′-diaminobenzidine tetrachloride (Sigma) in 0.05 M Tris buffer (pH 7.6) and 0.02% H_2O_2. Sections were mounted on gelatine-coated glass slides and coverslipped.

Following staining for GFAP, the sections were analyzed using an image analysis system (KS 400, Carl Zeiss Jena, Germany). Optical densities (OD) were measured in different regions of interest (ROI) in the dorsal horns. The region with the lowest immunoreactivity for GFAP was taken as the reference region (REF). Relative optical densities (ROD) were calculated as $ROD = [(OD_{ROI}/OD_{REF}) - 1] \times 100$. From each spinal cord, three to six sections were used for the calculations, and in each section, two to three regions were analyzed.

Statistical analysis of the difference between groups was done using a one-way ANOVA test; $P < 0.05$ was considered statistically significant. Data are expressed as mean ± S.E.M.

Results

Stimulation-evoked intrinsic optical signals and relative changes in ECS volume

Tetanic stimulation of the dorsal root (10 Hz for 1 min) evoked an increase in light transmittance (Fig. 2A), an increase in $[K^+]_e$, and a relative decrease in ECS volume, recorded as an increase in TMA^+ baseline concentration. The spatiotemporal distribution of the light transmittance response is shown in Fig. 2B. The peak amplitude of the light transmittance response was 6–8%, due to the variable size of the attached dorsal root. $[K^+]_e$ increased in the dorsal horn during stimulation to 6–8 mM, and its changes were generally faster than those in light transmittance (Fig. 2C). For measuring changes in ECS volume, the slices were superfused with a solution containing 1 mM TMA^+ chloride. Figure 2C demonstrates the TMA^+ baseline concentration increase of 0.04–0.05 mM during afferent stimulation in lamina III–V. The ECS volume shrinkage, evaluated from the TMA^+ baseline concentration increase assuming

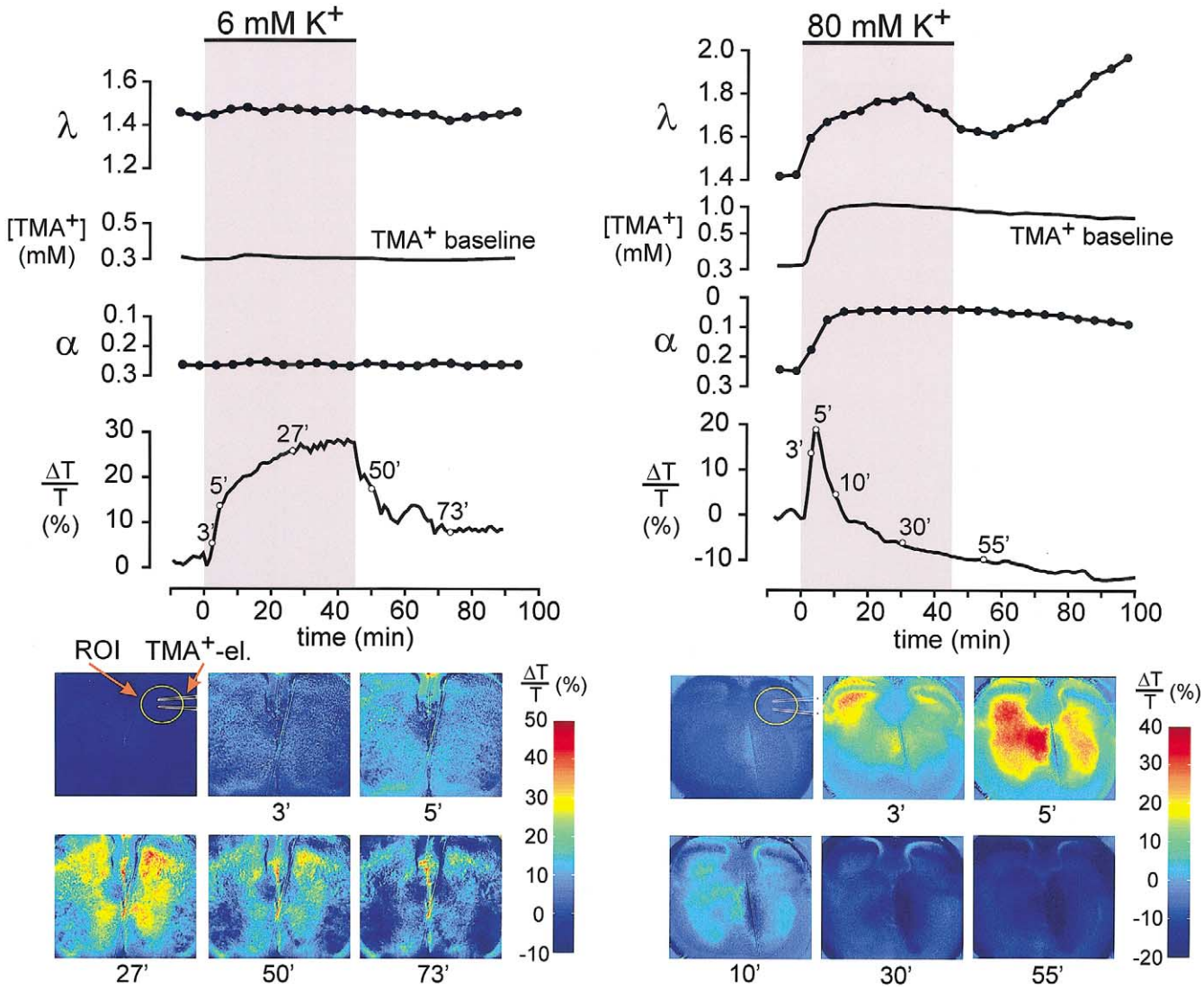

Fig. 4. The effect of 6 or 80 mM K^+ on the ECS diffusion parameters volume fraction α and tortuosity λ, the TMA^+ baseline and light transmittance. Changes in light transmittance in the selected area (see first video image) were plotted as a function of time. During the application of 80 mM K^+, the increase in light transmittance was substantially faster than the increase in α and, after reaching a peak, light transmittance decreased below control levels. Numbers below images indicate minutes after the application of 6 or 80 mM K^+.

that TMA^+ ions are restricted to the ECS, was therefore less than 5%. As is apparent from Fig. 2C, even though both the TMA^+ baseline concentration and light transmittance showed a rapid increase after the onset of the stimulation, the time courses did not correspond. Figure 2C also shows that the monitoring of relative ECS volume changes by using TMA^+ baseline changes has good time-resolution, but it does not allow the ECS volume to be accurately determined during fast focal changes as TMA^+ diffuses away from the area of its increased concentration. This problem can be surmounted by the generation of TMA^+ diffusion curves and the calculation of the absolute values of α, λ, and k', i.e., by a method that corrects for the loss of diffusing molecules by the introduction of a nonspecific uptake factor, k'.

Light transmittance and ECS diffusion parameter changes evoked by elevated K^+ or anisoosmotic solutions

In order to more accurately compare cell swelling and light transmittance changes, we used stimuli evoking longer and larger cell swelling, namely increased concentrations of K^+, anisoosmotic solutions, or the application of NMDA. Figure 3 shows diffusion curves obtained in spinal dorsal horn. An increase in the amplitude of the normalized curves reflects a decrease in the ECS volume fraction α, and an increase in the rise and decay time corresponds to an increase in tortuosity λ, i.e., an increase in diffusion barriers resulting from structural changes. An increase in tortuosity has been shown in our previous studies to be related particularly to reactive and hypertrophied astrocytes and the

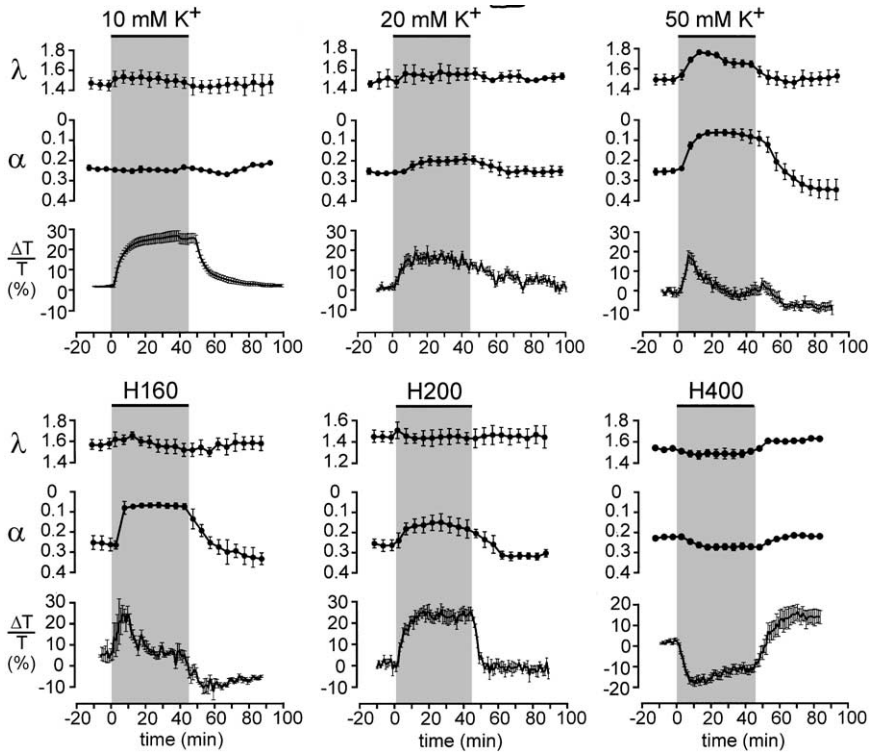

Fig. 5. Changes in the ECS diffusion parameters α and λ and changes in light transmittance evoked by increased potassium concentrations (10, 20, or 50 mM) or by osmotic stress (160, 200, or 400 mml/kg). Each data point represents mean ± S.E.M. ($n = 4–5$); α and λ values were determined at 5-min intervals and light transmittance, expressed as a percentage of change ($\Delta T/T\%$), at 1-min intervals. Note the different time course of change in ECS volume and light transmittance in all these typical recordings. Even if no cell swelling was evoked, i.e., during the application of 10 mM K^+, there was a large increase in light transmittance. The application of hypotonic (H200) or hypertonic (H400) solutions led to concomitant changes in α and light transmittance; however, the light transmittance changes reached their maximum substantially faster. During the large swelling-induced decrease in α induced by 50 mM K^+ or H160, light transmittance decreased after an initial peak to control levels, while shrinkage of the ECS persisted.

"crowding" of molecules of the extracellular matrix (Roitbak and Syková, 1999; Syková et al., 2000; Syková, 2001; Vargová et al., 2001). The diffusion curves superimposed on the changed TMA^+ baseline were recorded regularly at 5-min intervals. Using the three methods illustrated in Fig. 1, we could precisely follow the time course of cell swelling (TMA^+ baseline change), the time course of changes in the ECS diffusion parameters α and λ, and neuronal activity (rise in $[K^+]_e$), as well as determine the absolute values of ECS volume and tortuosity following experimental procedures.

In slices of various thickness (200, 400, 600, 800, and 1000 μm), the amplitude and time course of light transmittance changes were not different, but the thicker the slice, the smaller the signal/noise ratio. We therefore used slices 400-μm thick in order to have sufficient tissue thickness to measure ECS diffusion parameters using TMA^+-ISMs placed 100–180 μm distant from the iontophoretic (point) source of TMA^+. During superfusion of the spinal cord slice with normal artificial cerebrospinal fluid, ECS diffusion parameters were: $\alpha = 0.25 \pm 0.01$, $\lambda = 1.52 \pm 0.01$, and $k' = 5.71 \pm 0.54$ (mean ± S.E.M., $n = 62$). Figure 4 shows that there were regional differences in light transmittance in response to the application of high K^+, often with the largest response in the dorsal horn and the intermediate zone (20–25%) containing small neurons responding to noxious and sensitive afferent stimuli, many interneurons and fine afferent fibers, the smallest response in the ventral horn with groups of large motor neurons, and no apparent response in the white matter consisting of ascending and descending mainly myelinated axons. These differences were not dependent on whether the solutions first reached the ventral or dorsal horn. Figures 4 and 5 further show that the light transmittance increases in 6 or 10 mM K^+ persisted during 45 min of application and were larger than the light transmittance changes evoked by 20, 50, or 80 mM K^+, which reached a peak quickly and then returned toward the control level, often undershooting it. The application of 6 or 10 mM K^+, which evoked a large light transmittance increase, did not result in either an ECS volume decrease or an increase in tortuosity.

Time course of light transmittance and ECS volume changes evoked by elevated K^+ and by anisoosmotic solutions

In measurements in which changes in both light transmittance and TMA^+ diffusion curves were recorded, the

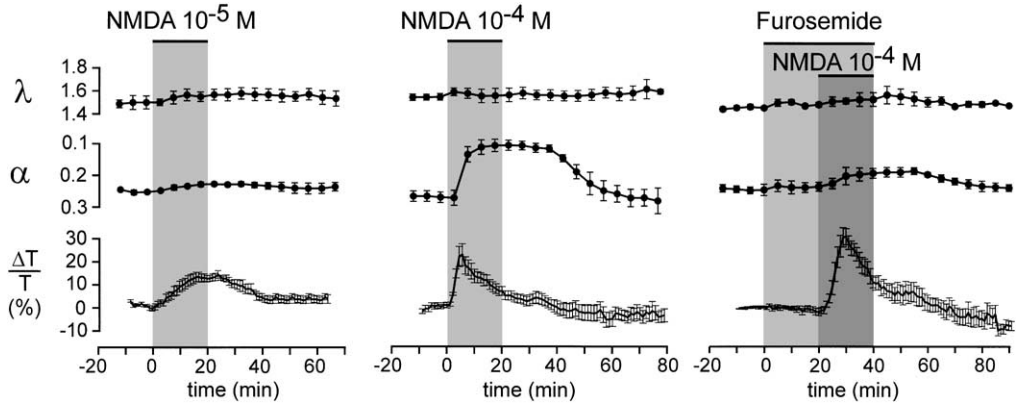

Fig. 6. The effect of glutamate receptor activation by the application of NMDA (10^{-5} or 10^{-4} M). Similarly, at low K^+ concentrations, the application of 10^{-5} M NMDA did not evoke any change in ECS diffusion parameters but did increase light transmittance. In contrast, 10^{-4} M NMDA induced a dramatic decrease in α, which persisted even 20 min after the application, while the light transmittance increase was faster and, after reaching a maximum, quickly returned to control levels. Furosemide (2 mM) blocked the NMDA-evoked decrease in α, while light transmittance remained unchanged.

time course of the light transmittance increase was faster than that of the decrease in the ECS volume fraction. Figures 4 and 5 show typical responses to a 45-min application of 20, 50, or 80 mM K^+. The application of 20 mM K^+ resulted in about a 20% increase in light transmittance, a small effect on ECS volume, and a small or no effect on tortuosity. Both 50 and 80 mM K^+ evoked changes in both light transmittance and ECS diffusion parameters, but the time courses of the changes were different. The increase in light transmittance in response to high K^+ concentrations was faster than the changes in ECS volume fraction and tortuosity. While the light transmittance increase reached its peak in 5–7 min, the changes in α and λ peaked in 15–25 min. In 50 mM K^+, light transmittance returned to control values after 15–20 min, while α remained decreased. In 80 mM K^+, light transmittance returned to control values even faster (12 min), α decreased to about 0.04, and λ increased to about 1.8 without any sign of recovery, resembling the situation after ischemic damage (Vargová et al., 2001). Figure 4 further shows that after about 15 min of a continuous application of 80 mM K^+, light transmittance decreased below control values, and this light transmittance undershoot lasted for more than 60 min, i.e., the change was irreversible. During the light transmittance undershoot, α did not change further, but λ continued to increase to values above 2.0. There was also a light transmittance undershoot after the application of 50 mM K^+ (Fig. 5).

Figure 5 demonstrates that the higher the concentration of K^+, the lower the α and the higher the λ. On the other hand, independent of the K^+ concentration, light transmittance showed the same percentage change, or even a smaller change with increasing K^+ concentration, apparently because the rise time was faster. Note that in both 6 and 10 mM K^+, α and λ were not changed, while there was a change in light transmittance of about 25%. It is therefore evident from Figs. 4 and 5 that there are two types of light transmittance responses. The increase in light transmittance was independent of changes in the ECS diffusion parameters; in fact, cell swelling was associated with a light transmittance decrease. The light transmittance undershoot seems to be associated with a second large increase in λ and might therefore be related to either irreversible structural changes or to astrogliosis, leading to an increase in ECS diffusion barriers (Roitbak and Syková, 1999; Syková et al., 2000; Syková, 2001; Vargová et al., 2001).

Similar discrepancies between a light transmittance increase and an extracellular space volume fraction decrease were found during the application of two hypotonic solutions, H160 and H200 (Fig. 5). H160 evoked a decrease in α to 0.08 and a fast light transmittance increase of about 20%, which reached its peak in 6–8 min, returned to control levels, and, in isoosmotic solution, was followed by a light transmittance undershoot. The application of H200 evoked a decrease in α to 0.15, no apparent change in λ, and a light transmittance increase of about 25%, which persisted throughout the whole period of application. The application of hypertonic solution H400 resulted in a small increase in α, a very small decrease in λ, and a decrease in light transmittance of almost 20%. After returning to isoosmotic artificial cerebrospinal fluid, there was a large light transmittance overshoot of 15–20% (Fig. 5).

Light transmittance, ECS volume changes, and the increase in extracellular K^+ evoked by NMDA

The application of NMDA evoked the largest and fastest responses in Rexed's laminae I–II and subsequently III–IV, including the substantia gelatinosa and nucleus proprius, containing neurons involved in pain, position, and light touch sensation. The application of NMDA at a concentration of 10^{-5} M evoked a light transmittance increase of about 15% but no detectable changes in α or λ (Fig. 6). Higher concentrations (10^{-4}) evoked a light transmittance increase of about 20–25% and a large decrease in α. However, the changes in light transmittance, α and λ evoked by NMDA had different time courses. NMDA at a concentra-

tion of 10^{-4} M evoked much faster light transmittance changes than the decrease in α. Figure 6 shows that similarly as in high K^+ or H160, the light transmittance increase reached a peak in about 5 min, while α decreased to 0.12 in about 10–15 min. There was often a small light transmittance undershoot during washout with artificial cerebrospinal fluid.

It has been shown in a number of studies that extracellular K^+ accumulation corresponds to spontaneous (Syková et al., 1974) or evoked neuronal activity (for review see Syková, 1992, 1997). Figure 7 shows that the light transmittance increase and the rise in extracellular K^+ displayed remarkably similar time courses if $[K^+]_e$ was recorded in the same region as light transmittance by K^+-ISM. There was not only a precise correlation of the peaks of both responses, but also a good correlation in the time course of both responses. K^+ accumulation was fastest and largest in the spinal dorsal horn region where the maximal light transmittance increase was found (Fig. 7).

Effect of furosemide, and Mg^{2+}-, Ca^{2+}-, and Cl^--free solutions

To further analyze the mechanisms involved in light transmittance changes, we used blockers of either cell swelling or neuronal activity. The major mechanism of glial swelling in the presence of increased K^+ concentrations involves carrier-mediated KCl–NaCl uptake and Donnan-mediated KCl fluxes (Kimelberg and Frangakis, 1985; Ballanyi et al., 1987; Walz, 1992). It was already shown in our previous study that furosemide, known to block cell swelling caused by $K^+/Na^+/2Cl^-$ cotransport, slows down and partly blocks the 50 mM K^+-evoked changes in α (Syková et al., 1999 and Fig. 8). In the present experiments, the application of furosemide did not affect the amplitude of the light transmittance increase evoked by 50 mM K^+, but it slowed down light transmittance recovery. Furosemide blocked the NMDA-evoked changes in α and λ, while the light transmittance increase was not affected (Fig. 6). Figure 8 further shows that Cl^--free solution blocked the decrease in α evoked by 50 mM K^+. However, Cl^--free solution by itself evoked a large increase in light transmittance that was associated with a 0.5 mM decrease in extracellular K^+. When 50 mM K^+ was applied in a Cl^--free solution, light transmittance increased by about 20%, but did not return to resting light transmittance levels, suggesting that cell swelling might be at least partly responsible for the light transmittance decrease. NMDA in a Cl^--free solution had no effect on the light transmittance increase, but it also did not evoke any changes in α nor any rise in extracellular K^+, suggesting that Cl^--free solution decreased neuronal excitability prior to the application of NMDA (Fig. 9).

Our previous studies have shown that the application of high Mg^{2+}, an NMDA channel blocker, or Ca^{2+}-free solution has no significant effect on the α and λ changes evoked by the application of 50 mM K^+ (Syková et al., 1999). The NMDA-evoked changes in ECS diffusion parameters were, however, blocked by Mg^{2+} and by Ca^{2+}-free solution (Vargová et al., 2001). Figures 8 and 9 show that Mg^{2+} had no effect on the changes in light transmittance or α evoked by 50 mM K^+, while the NMDA-evoked changes in light transmittance, α and extracellular K^+ were all blocked by 20 mM Mg^{2+}. While the changes in α and λ (Fig. 9) evoked by NMDA were blocked in Ca^{2+}-free solution (suggesting that extracellular Ca^{2+} is important for cellular, presumably glial, swelling), the light transmittance increase and extracellular K^+ accumulation remained unchanged.

Our results show that there is no correlation between a light transmittance increase and an ECS volume decrease due to cell swelling. In fact, our results show that extensive cell swelling is actually accompanied by a decrease in light transmittance (Figs. 4 and 5). Increases in light transmittance are clearly related to neuronal activity, which may lead to fine structural or morphological changes.

Morphological changes of astrocytes associated with light transmittance signals

It was demonstrated in our previous studies that the cell swelling induced by a 45–60 min application of 50-mM K^+, hypoosmotic solution, or glutamate receptor agonists is accompanied by astrogliosis and persistent changes in ECS tortuosity (Syková et al., 1999; Vargová et al., 2001). In this study we show that even the application of 6 or 10 mM K^+ (which facilitates neuronal activity and evoked an increase in light transmittance) is associated with changes in astrocyte morphology and GFAP expression. While no distinct increase in GFAP staining was observed after incubation with control artificial cerebrospinal fluid, incubation of the spinal cord in 6 or 10 mM K^+ for 45 min led to an increase in GFAP staining and to changes in glial cell morphology (Fig. 10). GFAP staining revealed astrocytes with thicker processes and more dense somata than in spinal cords incubated in normal artificial cerebrospinal fluid.

The mean relative optical density in spinal cord sections stained for GFAP was calculated. In control spinal cord slices ($n = 11$) incubated in artificial cerebrospinal fluid for 45 min, the mean relative optical density was $6.48 \pm 0.20\%$. In solutions with an increased concentration of extracellular potassium the mean relative optical density was significantly higher ($P < 0.05$). In 6, 10, and 50 mM K^+, the mean relative optical density increased to $10.21 \pm 0.30\%$ ($n = 11$), $17.67 \pm 0.50\%$ ($n = 8$), and $32.11 \pm 0.46\%$ ($n = 8$), respectively.

These data show that an increase in neuronal activity and a light transmittance increase, which can be evoked by relatively weak stimuli such as an increase in extracellular K^+ to 6 or 10 mM (concentrations that are often seen during adequate or electrical stimulation) that are not accompanied by cell swelling detectable with the TMA^+ method, can produce hypertrophy of astrocytic processes and, presumably, other fine morphological changes.

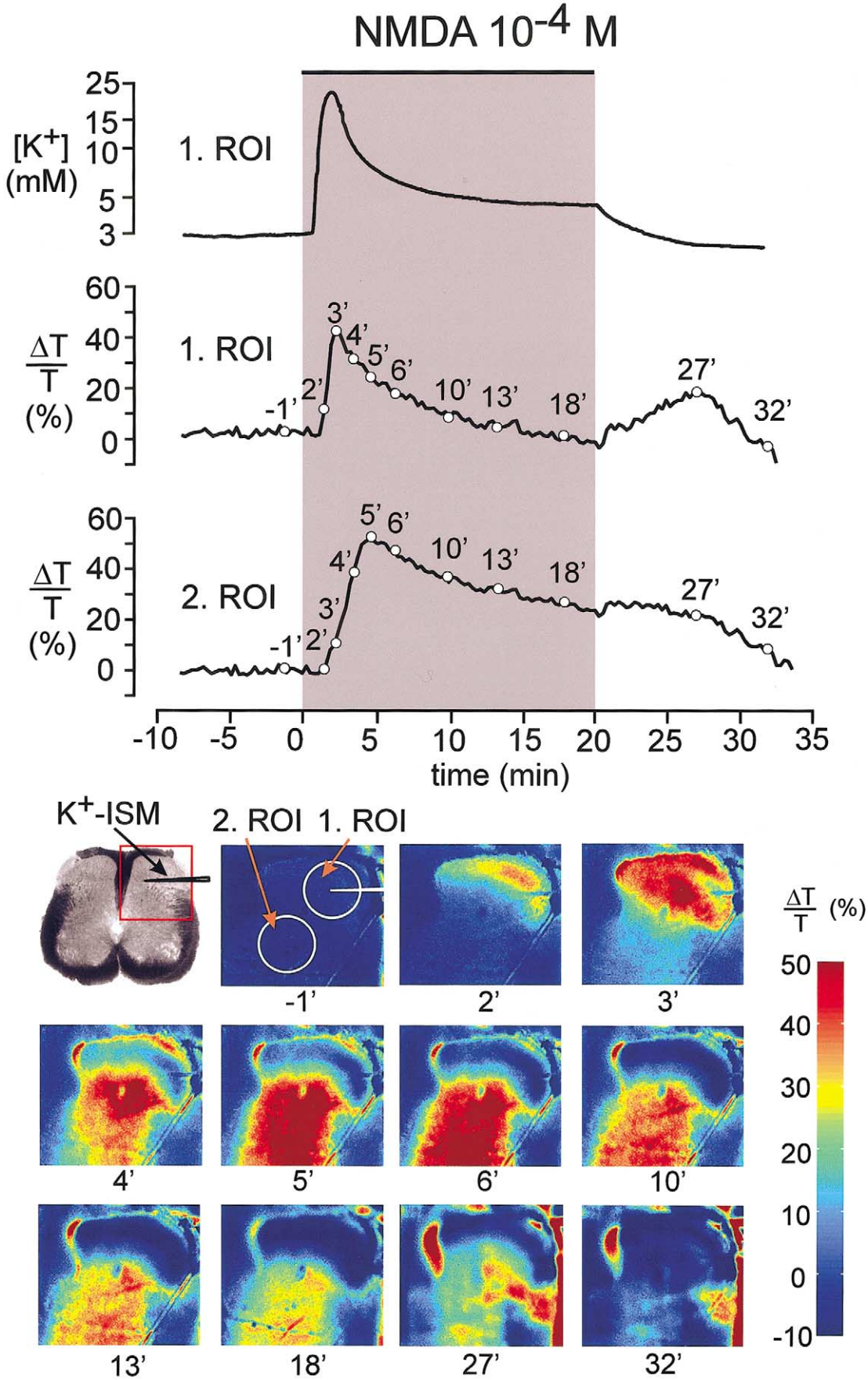

Fig. 7. Simultaneous measurements of $[K^+]_e$ changes and light transmittance during NMDA application. The first region of interest (1.ROI, Rexed's laminae I and II) corresponds to the insertion site of the K^+-ISM. The relatively fast increases in light transmittance and $[K^+]_e$ had similar time courses: they reached maximum values in about 5 min and then decreased toward the controls values. The increase in light transmittance in the second region of interest (2.ROI, Rexed's laminae IV and V) was significantly slower than the increase in light transmittance and $[K^+]_e$ in 1.ROI.

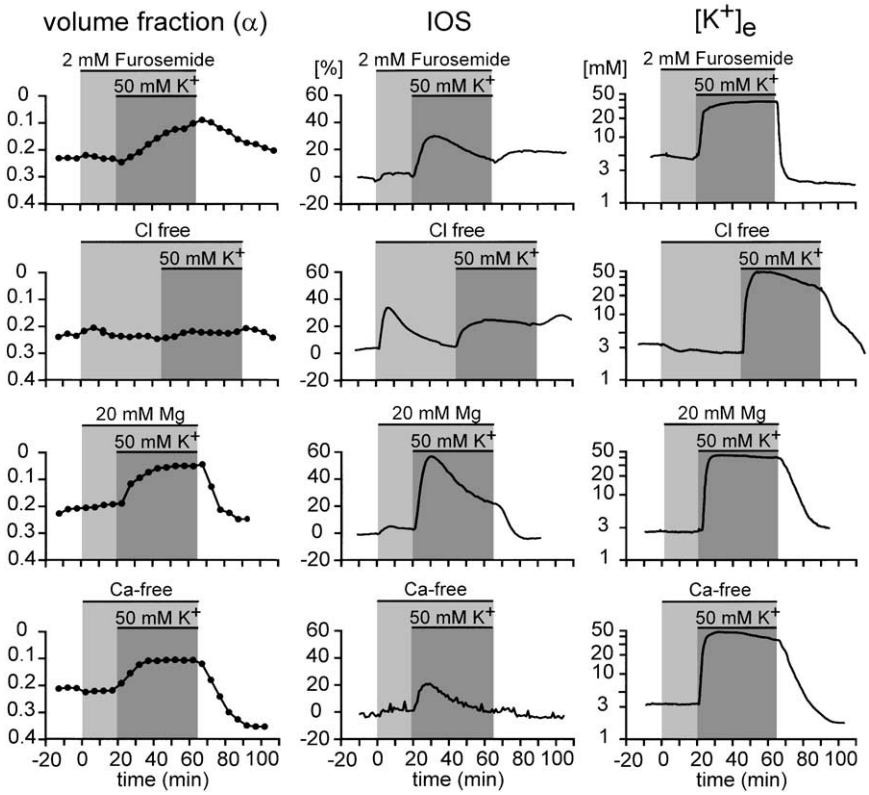

Fig. 8. Effect of furosemide, Cl-free solution, the NMDA channel blocker Mg^{2+}, and Ca-free solution on changes in ECS volume fraction (α), light transmittance, and $[K^+]_e$ recorded in the same ROI during the application of 50 mM K^+. Cl-free solution blocked, and furosemide (2 mM) slowed down, the α decrease and the recovery of light transmittance to control values evoked by the application of 50 mM K^+. Neither 20 mM Mg^{2+} nor Ca-free solution affected K^+-evoked cell swelling (α) or the light transmittance increase. Cl-free solution by itself led to an increase in light transmittance and a small decrease in $[K^+]_e$.

Discussion

The present study, performed on acute and relatively thick spinal cord slices, shows that there is no correlation between an increase in light transmittance and a decrease in ECS volume resulting from cell swelling. In fact, a larger light transmittance increase was evoked by various stimuli that do not produce cell swelling detectable by the real-time iontphoretic method, such as an increase in $[K^+]_e$ by 3 mM, low concentrations of glutamate receptor agonists, or electrical stimulation (Murase et al., 1998), than by stimuli that produce extensive cell swelling. Moreover, when cell swelling continued, light transmittance often decreased, apparently not due to water shift from the extra- to the intracellular compartment, but due to a block of neuronal activity resulting from a rise in $[K^+]_e$ above 12 mM or to receptor desensitization (see Syková, 1983, 1992).

Earlier studies performed in cell cultures have shown that the light-scattering signal is directly and linearly related to external osmolarity and to the cell volume, monitored by optical sectioning methods (Strange and Morrison, 1992). In addition, light scattering changed in a predictable manner when cells were exposed to media of varying osmolarity (Strange and Morrison, 1992). Recent studies performed on brain slices, however, indicate that light-transmittance and light-scattering changes in the CNS may not be correlated with cell swelling (Müller and Somjen, 1999) and that they may be affected by a number of other biophysical parameters of the nervous tissue besides cell volume changes (Jarvis et al., 1999).

Osmotic stress and light transmittance changes

Studies performed on glial cells in culture using morphological analysis, light scattering, flow cytometry, or fluorescence techniques have shown that a hypoosmotic solution produces cell swelling, while the application of a hyperosmotic solution results in cell shrinkage (Flögel et al., 1995; Tomita et al., 1994; McManus and Strange, 1993; Del Bigio et al., 1992; Eriksson et al., 1992). Studies performed on brain slices in situ, however, indicate that the effect of osmotic stress is more complicated. It was shown in the study of Andrew and MacVicar (1994) that light transmittance during cell swelling evoked by hypoosmotic solution increased in a linear fashion and was proportional to the strength of the hypoosmotic challenge. On the other hand, a hyperosmotic solution containing mannitol decreased light transmittance, while a hyperosmotic solution of the same ionic strength containing glycerol did not affect light transmittance (Andrew and MacVicar, 1994). In our experi-

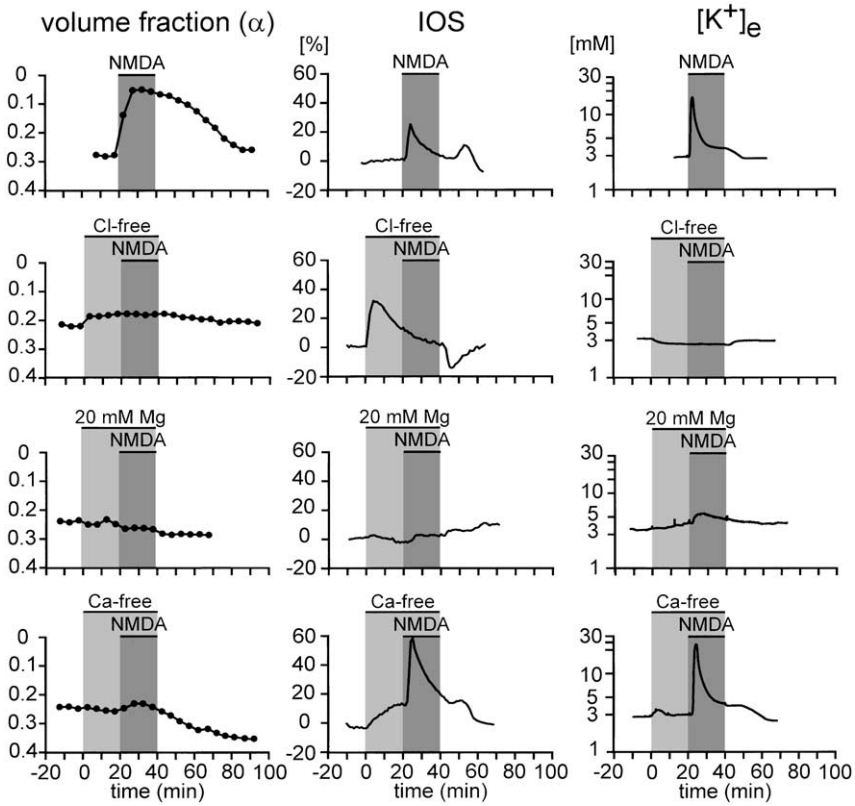

Fig. 9. Effect of Cl-free solution, Mg^{2+} and Ca-free solution on changes in ECS volume (α), light transmittance, and $[K^+]_e$ induced by the application of 10^{-4} M NMDA. The decrease in α, the increase in light transmittance, and the increase in $[K^+]_e$ evoked by NMDA application were suppressed in Cl-free solution. Twenty millimolar Mg^{2+} blocked changes in α, light transmittance, and $[K^+]_e$. In Ca-free solution, cell swelling (a decrease in α) was blocked, but the increases in light transmittance and $[K^+]_e$ persisted.

ments, hypotonic solutions decreased the ECS volume fraction as was shown previously (Syková et al., 1999), but the time course of changes in the ECS volume fraction did not correspond to the increase in light transmittance. This was particularly evident in a solution with a lower osmotic strength (H160), when the increase in light transmittance reached a peak before the ECS volume fraction substantially changed, suggesting that the light transmittance increase could not reflect only changes in cell volume. A similar study was recently performed on hippocampal slices exposed to hypotonic solutions, suggesting that at least one other mechanism besides cell swelling causes the light transmittance changes (Fayuk et al., 2002). In fact, the light transmittance increase was not proportional to the strength of the hypoosmotic challenge; the solution with a lower osmotic strength (H160) produced a smaller and shorter increase in light transmittance (Fig. 5). Similarly, the time course of the light transmittance decrease in hyperosmotic solution was faster than that of cell shrinkage (Fig. 5).

Effect of NMDA and high K^+

A number of studies have shown that glutamate receptors are present in neurons as well as in glial cells (Hollmann and Heinemann, 1994; Gallo and Russell, 1995; Steinhäuser and Gallo, 1996; Žiak et al., 1998). There is increasing evidence that glutamate evokes astrocytic swelling (Kimelberg, 1987; Chan et al., 1990; Hansson and Rönnbäck, 1994) and that such swelling is dependent on Cl^- and Ca^{2+} influx (Koyama et al., 1991; Vargová et al., 2001). Glial cells may swell in response to increased $[K^+]_e$, which accompanies the activation of glutamate receptors. Our previous study performed on isolated spinal cord has shown that glutamate receptor activation leads to an extracellular acid shift and to a transient increase of $[K^+]_e$ accompanied by cell swelling and a decrease in ECS volume (Vargová et al., 2001). In our experiments, the application of high K^+ or the glutamate receptor agonist NMDA evoked a concentration-dependent effect on the ECS diffusion parameters. However, the lower the concentration of K^+ or NMDA, the greater and longer was the increase in light transmittance. With a low concentration of K^+ (6 or 10 mM) or NMDA (up to 10^{-5} M), there were no changes in ECS volume fraction or tortuosity. High concentrations of K^+ (50–80 mM) or NMDA (10^{-4} M) evoked a prominent decrease in ECS volume fraction, which persisted for the whole duration of the application. However, an initial increase in light transmittance was followed by a decrease to control levels, even during the continued application of high K^+ or

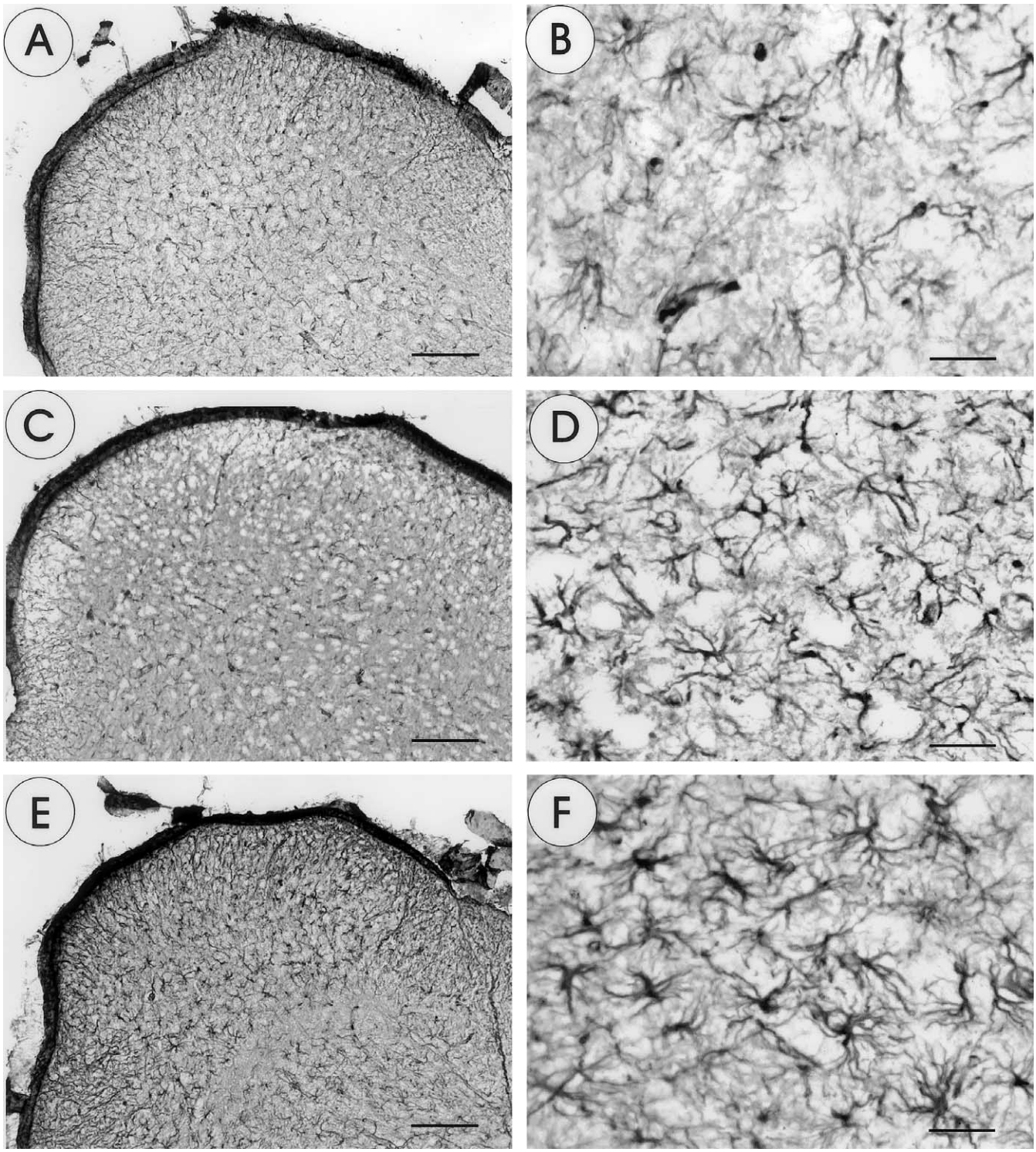

Fig. 10. GFAP staining of spinal cord slices of a 10-day-old rat incubated for 45 min in artificial cerebrospinal fluid (A, B), 6 mM K^+ (C, D), or 10 mM K^+ (E, F). Note that even incubation in low potassium concentrations resulted in astrocytic hypertrophy manifested as thicker processes, more dense somata, and increased GFAP staining. Scale bars = 100 μm (A, C, E) or 25 μm (B, D, F).

NMDA. While the increases in light transmittance clearly did not correspond to the changes in ECS volume fraction, they had a similar time course as did the increase in $[K^+]_e$ resulting from neuronal activity. A common origin for the K^+ increase and the light transmittance increase is supported by our finding that blocking synaptic activity with 20 mM Mg^{2+} resulted in a block of the K^+ rise as well as the light transmittance increase.

Previous studies performed on cultured astrocytes have shown that the application of high potassium induces cell swelling (for review see Kimelberg and Frangakis, 1985; Kimelberg and Ransom, 1986). K^+-induced astrocytic swelling may therefore result from a net KCl uptake via Na/K/2Cl cotransport and concomitant water influx into cells (Syková et al., 1999). A similar swelling mechanism also contributes to the decrease in ECS volume observed during the application of glutamate receptor agonists, which is accompanied by a large increase in $[K^+]_e$ (Vargová et al., 2001). In the present study, disruption of the astrocytic Na/K/2Cl cotransport system by furosemide or by Cl^--free solution diminished cell swelling (Figs. 6 and 8), but did not block the light transmittance increase evoked by NMDA or by 50 mM K^+. Our data are in agreement with experiments performed by Jarvis et al., (1999) in which an increase in light transmittance was found in control hippocampal slices as well as in slices perfused with furosemide. These authors suggested that an important contributor to these light transmittance changes could be some sort of neuronal changes leading to dendritic beading, which was shown to occur following seizures, exposure to glutamate or its agonists, ischemia, and electric stimulation. This dendritic beading may be associated with an increased number of light scatterers due to different dendritic shapes, and thus with a decrease in light transmittance (Jarvis et al., 1999). Such fine swelling of neuronal processes probably does not lead to substantial ECS volume changes, and it is therefore possible that rather fine structural changes are responsible for the increase in light transmittance. This is in agreement with our present finding showing large structural changes in astrocytic processes in all cases in which a light transmittance increase was found (see Fig. 10). Murase et al. (1998) reported in a rat spinal cord slice preparation a light transmittance increase evoked by the electrical stimulation of high-threshold primary afferent fibers. This light transmittance increase was abolished by the application of furosemide (Murase et al., 1998; Asai et al., 2002). Such a discrepancy may be explained by the direct effect of furosemide on primary afferent fibers, because such stimulation would lead to an accumulation of extracellular K^+ below 6 mM (Svoboda and Syková, 1991; Syková and Svoboda, 1990; Jendelová and Syková, 1991), and such changes do not result in vitro in changes of ECS volume or to cell swelling detectable by the TMA^+ real-time iontophoretic method.

It has been shown that activity-induced changes in intrinsic optical signals in rat cortical slices are associated with changes in ECS volume (Holthoff and Witte, 1996, 1998). However, these measurements of ECS volume changes were performed using TMA^+ baseline concentration recording. This method can properly monitor ECS volume changes only during the phase of rapid increase after the onset of stimulation, but it does not allow the correct determination of ECS volume due to artifacts caused by the diffusion of TMA^+ away from areas with a stimulation-increased concentration. In our experiments we also found stimulation-evoked cell swelling and an increase in light transmittance, but we did not observe a convincing correlation between these two responses.

It was suggested by experiments performed on cultured cells that the light scattered by a cell is directly proportional to the concentration of intracellular scatterers, and therefore shrinkage or swelling should cause an increase or decrease in the light-scattering signal (Fischbarg et al., 1989; Strange and Morrison, 1992). Earlier studies performed on brain slices also demonstrated activity-dependent increases in light transmittance across brain slices (associated with excitatory synaptic input and action potential discharge) and suggested that they are a consequence of glial and neuronal swelling or changes in the ECS evoked by cell swelling via a net KCl uptake and a concomitant water influx (Andrew and MacVicar, 1994; Andrew et al., 1999; Holthoff and Witte, 1996).

There is, however, increasing evidence that there is no simple correlation between intrinsic optical signal changes, cell swelling, and ECS volume changes. Meierkord et al. (1997) have shown that optical signal changes outlasted both seizure-like events and associated K^+ signals. In contrast, changes in ECS volume had a longer time course than the light transmission changes. These authors therefore suggested that even though ECS volume changes are widely held to be responsible for transmission changes, other mechanisms may also contribute to increased light transmission (Meierkord et al., 1997). In our experiments, the prominent light transmittance increases evoked by 6–10 mM K^+ or by 10^{-5} M NMDA were not accompanied by changes in the ECS volume fraction. However, even the application of 6 or 10 mM K^+ caused morphological changes in astrocytes, i.e., the hypertrophy of glial processes.

Light scattering in tissue is caused by the heterogeneity of the refractive index at the dimension of the wavelength. According to Bohren and Huffman (1983), the refractive index is determined by the magnetic permeability μ and the dielectric constant ε, which in tissue are affected by the concentrations of various particles including ions and macromolecules. Tao (2000) therefore suggested that any significant changes in the heterogeneity of particle concentrations at the wavelength dimension will alter the light scattering signal. Cell depolarization during neuronal activity and the accompanying ionic redistribution caused by the massive transmembrane ionic fluxes may increase the spatial fluctuation of ionic concentrations and thus affect light transmittance.

We conclude that the light transmittance increases in our study are associated with neuronal activity accompanied by various biochemical, biophysical, and morphological changes. Besides cell swelling, the changes at a subcellular level that affect how light penetrates tissue apparently include changes in fine glial and dendritic processes, dendritic spines, dendritic beads, axonal varicosities, swelling of cel-

lular organelles, the folding and unfolding of plasma membranes, and the refractive index of the cytoplasm.

Acknowledgments

We thank Ivan Voříšek for his participation in our preliminary experiments. This study was supported by Grants GACR 305/02/1528. GACR 309/00/1430, AV0Z5039906, MSMT LN00A065, and MSMT J13/98111300004.

References

Andrew, R.D., MacVicar, B.A., 1994. Imaging cell volume changes and neuronal excitation in the hippocampal slice. Neuroscience 62, 371–383.

Andrew, R.D., Adams, J.R., Polischuk, T.M., 1996. Imaging NMDA- and kainate-induced intrinsic optical signals from the hippocampal slice. J. Neurophysiol. 76, 2707–2717.

Andrew, R.D., Jarvis, C.R., Obeidat, A.S., 1999. Potential sources of intrinsic optical signals imaged in live brain slices. Meth. Enzymol. 18, 185–196.

Asai, T., Kusudo, K., Ikeda, H., Murase, K., 2002. Intrinsic optical signals in the dorsal horn of rat spinal cord slices elicited by brief repetitive stimulation. Eur. J. Neurosci. 15, 1737–1746.

Ballanyi, K., Grafe, P., ten Bruggencate, G., 1987. Ion activities and potassium uptake mechanisms of glial cells in guinea-pig olfactory cortex slices. J. Physiol. (Lond.) 3820, 1590–1740.

Bohren, C.F., Huffman, D.R., 1983. Absorbtion and Scattering of Light by Small Particles. Wiley, New York.

Chan, P.H., Chu, L., Chen, S., 1990. Effects of MK-801 on glutamate-induced swelling of astrocytes in primary cell culture. J. Neurosci. Res. 25, 87–93.

Cohen, L.B., Keynes, R.D., Hille, B., 1968. Light scattering and birefringence changes during nerve activity. Nature 218, 438–441.

Cohen, L.B., Keynes, R.D., Landowne, D., 1972a. Changes in light scattering that accompany the action potential in squid giant axons: potential-dependent components. J. Physiol. (Lond.) 224, 701–725.

Cohen, L.B., Keynes, R.D., Landowne, D., 1972b. Changes in axon light scattering that acconpany the action potential: current dependent components. J. Physiol. (Lond.) 224, 727–752.

Del Bigio, M.R., Fedoroff, S., Qualtiere, L.F., 1992. Morphology of astroglia in colony cultures following transient exposure to potassium ion, hypoosmolarity and vasopressin. J. Neurocytol. 21, 7–18.

Eriksson, P.S., Nilsson, M., Wagberg, M., Rönnbäck, L., Hansson, E., 1992. Volume regulation of single astroglial cells in primary culture. Neurosci. Lett. 143, 195–199.

Fayuk, D., Aitken, P.G., Somjen, G.G., Turner, D.A., 2002. Two different mechanisms underlie reversible, intrinsic optical signals in rat hippocampal slices. J. Neurophysiol. 87, 1924–1937.

Fischbarg, J., Kuang, K., Hirsch, J., Lecuona, S., Rogozinski, L., Silverstein, S.C., Loike, J., 1989. Evidence that the glucose transporter serves as a water channel in J774 macrophages. Proc. Natl. Acad. Sci. USA 86, 8397–8401.

Flögel, U., Niendorf, T., Serkowa, N., Brand, A., Henke, J., Leibfritz, D., 1995. Changes in organic solutes, volume, energy state, and metabolism associated with osmotic stress in a glial cell line: A multinuclear NMR study. Neurochem. Res. 20, 793–802.

Gallo, V., Russell, J.T., 1995. Excitatory amino acid receptors in glia: Different subtypes for distinct functions? J. Neurosci. Res. 42, 1–8.

Grinvald, A., Frostig, R.D., Lieke, E., Hildesheim, R., 1988. Optical imaging of neuronal activity. Physiol. Rev. 68, 1285–1366.

Hansson, E., Rönnbäck, L., 1994. Astroglial modulation of synaptic transmission. Perspect. Dev. Neurobiol. 2, 217–223.

Hill, D.K., Keynes, R.D., 1949. Opacity changes in stimulated nerve. J. Physiol. (Lond.) 108, 278–281.

Hollmann, M., Heinemann, S., 1994. Cloned glutamate receptors. Ann. Rev. Neurosci. 17, 31–108.

Holthoff, K., Witte, O.W., 1996. Intrinsic optical signals in rat neocortical slices measured with near-infrared dark-field microscopy reveal changes in extracellular space. J. Neurosci. 16, 2740–2749.

Holthoff, K., Witte, O.W., 1998. Intrinsic optical signals in vitro: A tool to measure alterations in extracellular space with two-dimensional resolution. Brain Res. Bull. 47, 649–655.

Jarvis, C., Lilge, L., Vipond, G.J., Andrew, R.D., 1999. Interpretation of intrinsic optical signals and calcein fluorescence during acute excitotoxic insult in the hippocampal slice. NeuroImage 10, 357–372.

Jendelová, P., Syková, E., 1991. Role of glia in K^+ and pH homeostasis in the neonatal rat spinal cord. Glia 4, 56–63.

Kimelberg, H.K., 1987. Anisotonic media and glutamate-induced ion transport and volume responses in primary astrocyte cultures. J. Physiol. (Paris) 82, 294–303.

Kimelberg, H.K., Frangakis, M.V., 1985. Furosemide a bumetamide-sensitive ion transport and volume control in primary astrocyte cultures from rat brain. Brain Res. 361, 125–134.

Kimelberg, H.K., Ransom, B.R., 1986. Physiological and pathological aspects of astrocyte swelling. Federoff, S., Vernadakis, A. (Eds.), In Astrocytes: Cell Biology and Pathology of Astrocytes. Academic Press, New York, pp 129–166.

Koyama, Y., Baba, A., Iwata, H., 1991. L-Glutamate-induced swelling of cultured astrocytes is dependent on extracellular Ca^{2+}. Neurosci. Lett. 122, 210–212.

Kreisman, N.R., LaManna, J.C., Liao, S.C., Yeh, E.R., Alcala, J.R., 1995. Light transmittance as an index of cell volume in hippocampal slices: Optical differences of interfaced and submerged positions. Brain Res. 693, 179–186.

Lehmenkühler, A., Syková, E., Svoboda, J., Zilles, K., Nicholson, C., 1993. Extracellular space parameters in the rat neocortex and subcortical white matter during postnatal development determined by difusion analysis. Neuroscience 55, 339–351.

McManus, M.L., Strange, K., 1993. Acute volume regulation of brain cells in response to hypertonic challenge. Anesthesiology 78, 1132–1173.

MacVicar, B.A., Hochman, D., 1991. Imaging of synaptically evoked intrinsic optical signals in hippocampal slices. J. Neurosci. 11, 1458–1469.

Meierkord, H., Schuchmann, S., Buchheim, K., Heinemann, U., 1997. Optical imaging of low Mg^{2+}-induced spontaneous epileptiform activity in combined rat entorhinal cortex-hippocampal slices. NeuroReport 8, 1857–1861.

Müller, M., Somjen, G.G., 1999. Intrinsic optical signals in rat hippocampal slices during hypoxia-induced spreading depression-like depolarization. J. Neurophysiol. 82, 1818–1831.

Murase, K., Saka, T., Terao, S., Ikeda, H., Asai, T., 1998. Slow intrinsic optical signals in the rat spinal dorsal horn in slice. NeuroReport 9, 3663–3667.

Nicholson, C., Phillips, J.M., 1981. Ion diffusion modified by tortuosity and volume fraction in the extracellular microenvironment of the rat cerebellum. J. Physiol. (Lond.) 321, 225–257.

Nicholson, C., Syková, E., 1998. Extracellular space structure revealed by diffusion analysis. Trends Neurosci. 21, 207–215.

Prokopová-Kubinová, Š., Syková, E., 2000. Extracellular diffusion parameters in spinal cord and filum terminale of the frog. J. Neurosci. Res. 62 (4), 530–538.

Rector, D.M., Poe, G.R., Kristensen, M.P., Harper, R.M., 1997. Light scattering changes follow evoked potentials from hippocampal Schaeffer collateral stimulation. J. Neurophysiol. 28, 1707–1713.

Rector, D.M., Rogers, R.F., Schwaber, J.S., Harper, R.M., George, J.S., 2001. Scattered-light images *in vivo* tracks fast and slow processes of neurophysiological activation. NeuroImage 14, 977–994.

Roitbak, T., Syková, E., 1999. Diffusion barriers evoked in the rat cortex by reactive astrogliosis. Glia 28, 40–48.

Steinhäuser, C., Gallo, V., 1996. News on glutamate receptors in glial cells. Trends Neurosci. 19, 339–345.

Strange, K., Morrison, R., 1992. Volume regulation during recovery from chronic hypertonicity in brain glial cells. Am. J. Physiol. 263, C412–C419.

Svoboda, J., Syková, E., 1991. Extracellular space volume changes in the rat spinal cord produced by nerve stimulation and peripheral injury. Brain Res. 560, 216–224.

Syková, E., 1983. Extracellular K^+ accumulation in the central nervous system. Prog. Biophys. Mol. Biol. 42, 135–189.

Syková, E., 1992. Ionic and volume changes in the microenvironment of nerve and receptor cells. D., Ottoson (Ed.), In Progress in Sensory Physiology, vol. 13. Springer, Heidelberg, pp. 1–176.

Syková, E., 1997. The extracellular space in the CNS: its regulation, volume and geometry in normal and pathological neuronal function. Neuroscientist 3, 28–41.

Syková, E., 2001. Glial diffusion barriers during aging and pathological states. Prog. Brain Res. 132, 339–363.

Syková, E., Svoboda, J., 1990. Extracellular alkaline–acid–alkaline transients in the rat spinal cord evoked by peripheral stimulation. Brain Res. 512, 181–189.

Syková, E., Rothenberg, S., Krekule, I., 1974. Changes of extracellular potassium concentration during spontaneous activity in the mesencephalic reticular formation of the rat. Brain Res. 79, 333–337.

Syková, E., Svoboda, J., Polák, J., Chvátal, A., 1994. Extracellular volume fraction and diffusion characteristics during progressive ischemia and terminal anoxia in the spinal cord of the rat. J. Cereb. Blood Flow Metab. 14, 301–311.

Syková, E., Mazel, T., Šimonová, Z., 1998. Diffusion constraints and neuron–glia interaction during aging. Exp. Gerontol. 33, 837–851.

Syková, E., Vargová, L., Prokopová, Š., Šimonová, Z., 1999. Glial swelling and astrogliosis produce diffusion barriers in the rat spinal cord. Glia 25, 56–70.

Syková, E., Mazel, T., Vargová, L., Vořišek, I., Prokopová, Š., 2000. Extracellular space diffusion and pathological states. Prog. Brain Res. 125, 155–178.

Tao, L., 2000. Light scattering in brain slices measured with a photon counting fiber optic system. J. Neurosci. Meth. 101, 19–29.

Tasaki, I., Byrne, P.M., 1993. The origin of rapid changes in birefringence, light scattering and dye absorbance associated with excitation of nerve fibers. Jpn. J. Physiol. 43, S67–S75.

Tomita, M., Fukuuchi, Y., Terakawa, S., 1994. Differential behavior of glial and neuronal cells exposed to hypotonic solution. Acta Neurochir. 60, 31–33.

Vargová, L., Jendelová, P., Chvátal, A., Syková, E., 2001. Glutamate, NMDA and AMPA induced changes in extracellular space volume and tortuosity in the rat spinal cord. J. Cereb. Blood Flow Metab. 21, 1077–1089.

Walz, W., 1992. Mechanism of rapid K^+-induced swelling of mouse astrocytes. Neurosci. Lett. 135, 243–246.

Žiak, D., Chvátal, A., Syková, E., 1998. Glutamate-, kainate- and NMDA-evoked membrane currents in identified glial cells in rat spinal cord slice. Physiol. Res. 47, 365–375.